Food Chemistry: X 25 (2025) 102164

Contents lists available at ScienceDirect

Food Chemistry: X

journal homepage: www.sciencedirect.com/journal/food-chemistry-x

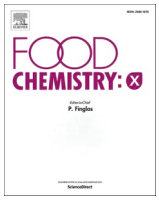

Exopolysaccharides from camel milk-derived *Limosilactobacillus reuteri* C66: Structural characterization, bioactive and rheological properties for food applications

A.K.M. Humayun Kober [a,1], Mohamed Abdin [b,1], Athira Subhash [b], Shao-Quan Liu [c], Enes Dertli [d], Basim Abu-Jdayil [e], Pau-Loke Show [f], Mutamed Ayyash [b,*]

[a] Department of Dairy & Poultry Science, Chattogram Veterinary and Animal Sciences University, Khulshi, Chittagong 4225, Bangladesh
[b] Department of Food Science, College of Agriculture and Veterinary Medicine, United Arab Emirates University (UAEU), Al Ain, United Arab Emirates
[c] Department of Food Science and Technology, Faculty of Science, National University of Singapore, Singapore 117542, Singapore
[d] Department of Food Engineering, Faculty of Chemical and Metallurgical Engineering, Yildiz Technical University, İstanbul, Turkey
[e] Chemical and Petroleum Engineering Department, College of Engineering, United Arab Emirates University (UAEU), Al Ain, United Arab Emirates
[f] Department of Chemical Engineering, Khalifa University, Abu Dhabi, Abu Dhabi Municipality, United Arab Emirates

ARTICLE INFO

Keywords:
Exopolysaccharides
Limosilactobacillus reuteri
Rheological properties
ACE-inhibition
Antioxidants

ABSTRACT

Microbial exopolysaccharides (EPS) are valued as safe, functional bio-ingredients in food. Produced by microorganisms like lactic acid bacteria (LAB), they enhance the rheological and sensory properties of food products. In this study, *Limosilactobacillus reuteri* C66 (EPS-C66), was utilized to produce EPS. EPS-C66 was isolated, purified, and characterized for its rheological properties and biofunctionalities. Molecular weight was 3.7×10^5 Da. Three monosaccharides (arabinose, mannose, and glucose) were identified. At 10 mg/mL, EPS-C66 exhibited significant scavenging activity against DPPH and ABTS radicals, achieving 67.9 % and 31.3 %, respectively. Additionally, it reduced the viability of Caco-2 and MCF-7 cancer cells by 93.7 % and 61.4 %, respectively. EPS-C66 also demonstrated antibacterial effects against *S. aureus, S. typhimurium, L. monocytogenes,* and *E. coli,* with ranges of 5.9, 6.1, 6.0, and 5.7 log CFU/mL, respectively. The current study highlights that EPS-C66 can enhance the health benefits and rheological properties of foods, contributing to the development of novel functional foods.

1. Introduction

Microbial exopolysaccharides (EPS) are multifaceted molecules composed of repeated monosaccharide subunits and are produced outside the microbial cell. EPS are generally synthesized by a range of microorganisms including LAB and non-LAB, such as *Lactobacillus* and *Bifidobacterium* species (Nabot et al., 2022). They are especially well-suited for biotechnological applications in the food sector because they are generally recognized as safe (Saadat et al., 2019). Microbial EPSs differ primarily depending on the species and strains. Additional factors that could influence their characteristics include the composition of the medium, the culture environment, the structure of monosaccharides, charge, linkages between units, and the presence of repetitive side chains and substitutions.

EPS can be categorized into two primary types: homopolysaccharides, which are composed of a single type of sugar molecule, and heteropolysaccharides, which consist of several different sugar molecules (Zhang et al., 2024). EPS production mechanisms vary with microorganisms. *L. bulgaricus* and *S. thermophilus* utilize Wzx/Wzy-dependent pathways for homo-exopolysaccharide production while employing the extracellular synthetic pathway for heteropolysaccharide production (Zhou et al., 2021). These polysaccharides can alter the flavor, texture, and appearance of fermented foods. The viscoelastic properties of EPS, such as energy retention and release (especially storage (G') and loss (G") moduli), significantly impact their performance (Ayyash, Abu-Jdayil, Olaimat, et al., 2020).

The rheological properties of exopolysaccharides (EPS) vary due to differences in their molecular weight, the types of bonds between sugar

* Corresponding author.
E-mail addresses: akmhumayun@cvasu.ac.bd (A.K.M.H. Kober), mutamed.ayyash@uaeu.ac.ae (M. Ayyash).
[1] Both authors contributed equally to this manuscript

https://doi.org/10.1016/j.fochx.2025.102164
Received 18 September 2024; Received in revised form 30 November 2024; Accepted 5 January 2025
Available online 7 January 2025
2590-1575/© 2025 The Author(s). Published by Elsevier Ltd. This is an open access article under the CC BY-NC-ND license (http://creativecommons.org/licenses/by-nc-nd/4.0/).

molecules, the sugar composition, and the functional groups attached to them (Zhou et al., 2019). In the food industry, they are valuable for their ability to form gels, mix ingredients, and act as emulsifiers, stabilizers and thickeners.

EPS in dairy products improve thickness, stability, and texture by acting as thickening agents, enhancing water retention, and reducing syneresis. They also help retain water and fat, contributing to a creamier texture and higher yield without altering the taste (Xu et al., 2019b). Concerning the pharmaceutical sector, EPS has been utilized as an antioxidant, antibacterial, and antitumor agent (Ayyash, Abu-Jdayil, Itsaranuwat, et al., 2020; Jeong et al., 2017; Wang et al., 2015). Discovering natural compounds that can combat tumors, heart diseases, and diabetes is crucial to minimizing the negative impacts of numerous chemotherapy medications and preventing the body from developing resistance to specific drugs (Ayyash, Abu-Jdayil, Olaimat, et al., 2020). Dairy LABs contain a variety of bioactive compounds that could exert such protective effects. Consuming fermented probiotic dairy products may help prevent breast cancer, bladder cancer, stomach cancer, and colorectal cancer (Kober et al., 2024).

Although microbial exopolysaccharides (EPS) are gaining attention for their functional benefits in the food industry, research on the bioactive and rheological properties of EPS from L. *reuteri*, especially those derived from camel milk, remains limited. In contrast, EPS from other lactic acid bacteria, such as L. *casei*, have shown promising biofunctionalities, including antihypertensive effects through ACE inhibition (Sørensen et al., 2022), the EPS from L. *reuteri* remains understudied in this context. Few studies have explored the strain-dependent differences in EPS production and composition among L. *reuteri* strains (İspirli et al., 2019; Miao et al., 2015; Zhao et al., 2022), leaving a gap in understanding the specific functional properties of EPS produced by L. *reuteri* C66. Moreover, no comprehensive evaluation of both the rheological and bioactive properties, such as antioxidant, antibacterial, and anticancer activities, has been conducted for this strain.

Camel milk-derived *Limosilactobacillus reuteri* C66 exopolysaccharides (EPS) offer superior bio-functional and rheological properties compared to EPS from other sources, attributed to camel milk's unique biochemical composition, including high levels of bioactive peptides, lactoferrin, and essential minerals. These EPS exhibit potent α-amylase and α-glucosidase inhibition, highlighting their potential for managing diabetes by controlling postprandial glucose levels. Additionally, they possess strong antioxidant, antimicrobial, and cytotoxic activities, aligning with applications in pharmaceutical and functional food sectors. Compared to EPS from other lactic acid bacteria (LAB) such as L. *casei*, camel milk-derived EPS exhibit enhanced stability under extreme conditions and hypoallergenic properties, making them suitable for a broader consumer base (Bakry et al., 2021; Wu et al., 2023; Xu et al., 2019a; Zhang et al., 2023). Despite these advantages, strain-specific variations and comprehensive industrial evaluations remain underexplored, necessitating further research to fully harness their potential. A deeper evaluation of their performance in real-world food and pharmaceutical applications is needed, especially their interaction with other ingredients. Therefore, the present study was undertaken to characterize the EPS-C66 produced by a potential probiotic strain L. *reuteri* C66 isolated previously from camel milk and to assess its biological activities, including antioxidant capacity, amylase and glucosidase inhibition, ACE-inhibition, cytotoxicity, and antipathogenic activity. Furthermore, the study examined the rheological properties of EPS-C66 as influenced by different salts (NaCl and $CaCl_2$) and pH values (4.0 and 6.0).

2. Materials and methods

2.1. Bacteria and propagation

Limosilactobacillus reuteri C66 was isolated by Abushelaibi et al. (2017) and stored in a solution with 50 % glycerol at −80 °C. It was then grown in MRS broth (de Mann Rogosa Sharpe; LAB-M Limited, Lancashire, UK) at 37 °C for 20 h. After incubation, it was kept at 4 °C for short-term storage (less than a week). Two successive cultivations (37 °C/20 h in MRS broth) of L. *reuteri* C66 were performed before EPS extraction each time.

2.2. Isolation and purification of EPS-C66

The extraction of EPS from L. *reuteri* C66 fermented broth was achieved in three steps following the detailed procedure of Ayyash, Abu-Jdayil, Itsaranuwat, et al. (2020). Firstly, *L. reuteri* C66 was cultured in an MRS broth containing 20 g/L sucrose. Cell removal was achieved using centrifugation and filtration after incubating the inoculated M-17 broth at 25.0 ± 0.1 °C for 48 h and centrifuging at 4000 ×*g* for 20 min at 4 °C to obtain a cell-free supernatant (CFS). In the second step, a precipitating agent (chilled absolute ethanol) was added to precipitate the EPS from the CFS, followed by refrigeration at 4 °C for 24 h. The crude extract was then collected by centrifugation at 8000 ×*g* for 30 min at 4 °C. In the third step, the crude extract was mixed with trichloroacetic acid to achieve a final concentration of 8 %. The partially purified EPS was lyophilized at −80 °C, with some stored at −20 °C in a sealed container for later analysis. A sample was scanned for traces of nucleic acids and proteins using a UV–Vis spectrometer at 260 and 280 nm (Epoch2, Bio-Tek, VT, US) to detect DNA and protein traces, respectively. No absorbance was detected, indicating the absence of nucleic acids or proteins.

2.3. EPS characterization

2.3.1. Determination of average molecular mass and monosaccharide composition

EPS-C66 solution was filtered through 0.22 μm syringe filters before injection into the SIL-20 AC autosampler of the Shimadzu HPLC system (Kyoto 604–8511, Japan), equipped with a refractive index detector (RID-20 A) (Bamigbade et al., 2024). The EPS-C66 Mw was calculated using calibration curves derived from pullulan standards with molecular weights of 800, 400, 200, 110, 50, 22, 10, 6, 1.3, and 0.342 kDa. The monosaccharide composition of the EPS-C66 was assessed using the method reported by Bamigbade et al. (2024). In brief, the EPS-C66 was initially treated with 2 M trifluoroacetic acid for hydrolysis and then reacted with 1-phenyl-3-methyl-5-pyrazolone (PMP) for derivatization. The resulting derivatized MPS was then passed through a 0.45 μm membrane filter and introduced into the Shodex C18 column (250 × 4.6 mm, 5 μm) of the Shimadzu HPLC system. This system is fitted with an SPD-M20A photodiode array detector set at PDA-245 nm and runs on a gradient program with a variable mobile phase (A: 0.1 M ammonium acetate, B: acetonitrile), a flow rate of 1.5 mL/min, and a column temperature of 30 °C.

2.3.2. Fourier transform-infrared spectroscopy (FT-IR)

The infrared analysis for functional groups in the EPS of L. *reuteri* C66 was conducted using an attenuated total reflectance FT-IR spectrophotometer in the spectrum range of 400–4000 cm–1 at room temperature. A diamond/ZnSe crystal plate was used, and the EPS powder was positioned on the plate.

2.3.3. Nuclear magnetic resonance (NMR) analysis

NMR analysis was performed on an Avance III Bruker spectrometer operating at 600 MHz with a cryoprobe, following the procedure of Bubb (2003). One-dimensional spectra (^{1}H and ^{13}C) and two-dimensional spectra were used to determine total correlation spectroscopy and heteronuclear multiple bond correlation. The CASPER program (www.casper.organ.su.se/casper) was used to predict the EPS structure. The procedure and analysis were conducted as described previously (El-Deeb et al., 2018).

2.3.4. Thermal properties

A differential scanning calorimeter was used to assess how EPS reacts to different temperatures. A small amount (25 mg) of EPS was heated in a special dish from 20 °C to 350 °C. A thermogram was recorded following the previously explained protocol (Sasikumar et al., 2017).

2.3.5. Scanning electron microscopy (SEM)

Surface morphology of the EPS was analyzed using a scanning electron microscope (Akishima, Tokyo, Japan) operated at a high voltage (20 kV) to obtain high-resolution images. A small amount (5 mg) of EPS was air-dried and coated with gold using a Cressington 108 Auto Sputter Coater (Ted Pella Inc., Redding, CA, USA).

2.3.6. Zeta potential and particle size analysis

Zeta potential was measured to understand the surface charge and stability of the EPS. The analysis was performed using a Nano Plus Zeta potential and particle size analyzer (Particulate System, GA, USA) as per the previously described protocol (Sasikumar et al., 2017).

2.4. Evaluation of EPS bioactivities

2.4.1. Antioxidant capacity

The EPS was tested for its antioxidant capacity using *in vitro* 2,2-azino-bis (3-ethylbenzo-thiazoline-6-sulphonic acid) (ABTS) and 1,1-diphenyl-2-picrylhydrazyl (DPPH) radical scavenging assays (Ayyash, Abu-Jdayil, Olaimat, et al., 2020). The scavenging activity was evaluated at two different concentrations of EPS (5 and 10 mg/mL). The DPPH and ABTS scavenging activities were calculated using Eq. 1 to determine the percentages.

$$\text{Scavenging Rate } (\%) = \left[1 - \frac{A_{sample} - A_0}{A_{control} - A_0}\right] \times 100 \quad (1)$$

where A_0 is the blank absorbance (negative control). $A_{control}$ is the absorbance of the radical of Vitamin C as a positive control.

2.4.2. Cytotoxicity activity

The cytotoxicity activity of EPS was evaluated using Caco-2 and MCF-7 cells, derived from colon and breast cancers, respectively, at 5 and 10 mg/mL concentrations. The protocol utilized was thoroughly explained previously (Ayyash, Abu-Jdayil, Olaimat, et al., 2020). Cytotoxicity percentage was calculated using Eq. 2.

$$\text{Cytotoxicity } (\%) = \left[1 - \frac{R_{sample} - R_0}{R_{control} - R_0}\right] \times 100 \quad (2)$$

where R_{sample} is the absorbance ratio of OD570/OD605 of the EPS, $R_{control}$ is the absorbance of the control sample (without EPS) and R_o is the average background, considered as a negative control with no cells.

2.4.3. Antimicrobial activity

The antimicrobial activity of EPS produced by L. *reuteri* C66 was assayed against four foodborne pathogenic bacteria: *E. coli* O157, *Salmonella Typhimurium* 02–8423, *Listeria monocytogenes*, and *Staphylococcus aureus* ATCC 25923. The response of bacteria to higher EPS concentrations was examined, as mentioned previously (Jeong et al., 2017). A 100 µL solution of EPS (5 mg/mL) was combined with 250 µL of activated pathogen in brain heart infusion (BHI, LAB-M), then incubated at 37 °C for 18 h. The pathogen was then counted on BHI agar (LAB-M) and incubated aerobically at 37 °C for an additional 24 h.

$$\text{Inhibition } (\%) = \left(1 - \frac{Abs_{sample} - Abs_{blank}}{Abs_{control}}\right) \times 100 \quad (3)$$

where Abs_{sample}: OD of inoculated BHI with EPS, Abs_{blank}: OD of BHI with EPS but no bacteria, and $Abs_{control}$ of inoculated BHI without EPS.

2.4.4. Antidiabetic activity

The *in vitro* antidiabetic activity was assessed by determining the ability of the produced EPS to inhibit α-amylase and α-glucosidase. According to Ayyash, Abu-Jdayil, Olaimat, et al. (2020), the inhibition of the two enzymes was assessed using different concentrations of the new EPS. The inhibition percentage was calculated using Eq. 3. Where Abs_{sample}: OD of essay with EPS, Abs_{blank}: OD of essay without, and $Abs_{control}$ of essay without EPS (enzyme and substrate).

2.5. Rheological properties

After EPS-C66 samples were prepared, rheological tests were conducted using a Discovery Hybrid Rheometer (TA Instruments, New Castle, DE, US). Aqueous solutions were prepared by adding 0.1 M $CaCl_2$ or 0.1 M NaCl to a 5 mg/mL EPS-C66 aqueous solution. The solutions were adjusted to two pH values (pH 4.0 and pH 6.0). The rheological characteristics of the water-based solution were assessed using cone and plate geometries (with a 1° cone angle, 50 mm gap, and 50 mm diameter). The plate was kept at a constant temperature of 25.0 ± 0.1 °C.

2.5.1. Apparent viscosity

The flow characteristics of the prepared EPS-C66 solutions were evaluated for their response to varying shear rates (ranging from 10 s^{-1} to 1000 s^{-1}) in both upward and downward directions. The assessments were performed at a temperature of 25.0 ± 0.1 °C. The difference between the upward and downward curves was utilized to gauge the extent of thixotropy. The flow patterns of the innovative EPS were characterized using the power law model (Eq. 4).

$$\tau = mY\dot{}\eta\ldots \quad (4)$$

where τ is the shear stress, m is the consistency coefficient, $Y\dot{}$ is the shear rate, and η is the flow behavior index.

2.5.2. Temperature-dependent behavior

The apparent viscosity of the new EPS-C66 was evaluated by ramping up the temperature to 80 °C at a speed of 3 °C/min while maintaining a constant shear rate of 20 s^{-1}. The flow activation energy of EPS-C66 was computed using the Arrhenius equation (Eq. 5).

$$n = n_0 e \frac{E_a}{RT} \quad (5)$$

where n is the apparent viscosity, $n_0$is the Arrhenius constant, E_a is the flow activation energy, R is the gas constant, and T is the temperature in Kelvin.

2.5.3. Amplitude and frequency sweep tests

To assess the linear viscoelastic region of EPS-C66, a test measuring amplitude strain was conducted. This test utilized a consistent frequency of 1 Hz and explored strain levels ranging from 0.1 % to 20 %. Subsequently, a frequency sweep test was performed within a frequency spectrum of 0.1–20 Hz at a steady strain under 2 %, which falls within the linear viscoelastic range. This was to analyze the viscoelastic characteristics of EPS, specifically the storage modulus (G′), loss modulus (G″), and the damping factor (tan δ). Both the amplitude and frequency sweep tests were executed at a stable temperature of approximately 25.0 ± 0.1 °C.

2.6. Statistical analysis

All measurements were taken in triplicate during the experiments. A one-way ANOVA was applied to identify any significant differences between the data sets. The results were presented as mean values with their corresponding standard deviations (mean ± SD), and a significance level of $P < 0.05$ was used to determine statistical relevance. Fisher's test was conducted to compare the mean values at this

significance level.

3. Results and discussion

3.1. Molecular weight and monosaccharide composition of EPS-C66

To ascertain the biological and functional characteristics of EPS, it is crucial to investigate their chemical structure and content. The average molecular weight of EPS-C66 was determined to be 3.7 × 10^5 Da (Fig. 1A). This result is relatively comparable to the molecular weight of EPS produced by L. *reuteri* SK24.003 (2.5 × 10^7 Da) (Miao et al., 2015) and L. *reuteri* DSM 17938 (6.5 × 10^5 Da) (Kšonžeková et al., 2016). The larger molecular weight significantly contributes to the rheological properties and viscosity of food products (Zhou et al., 2019). As illustrated in Fig. 1B and C, EPS-C66 is composed of three monosaccharides: mannose, glucose, and galactose in a molar ratio of 1.0:9.5:0.5. This variation in monosaccharides shows that EPS-C66 is a hetero-EPS. The monosaccharide composition significantly influences the functionalities

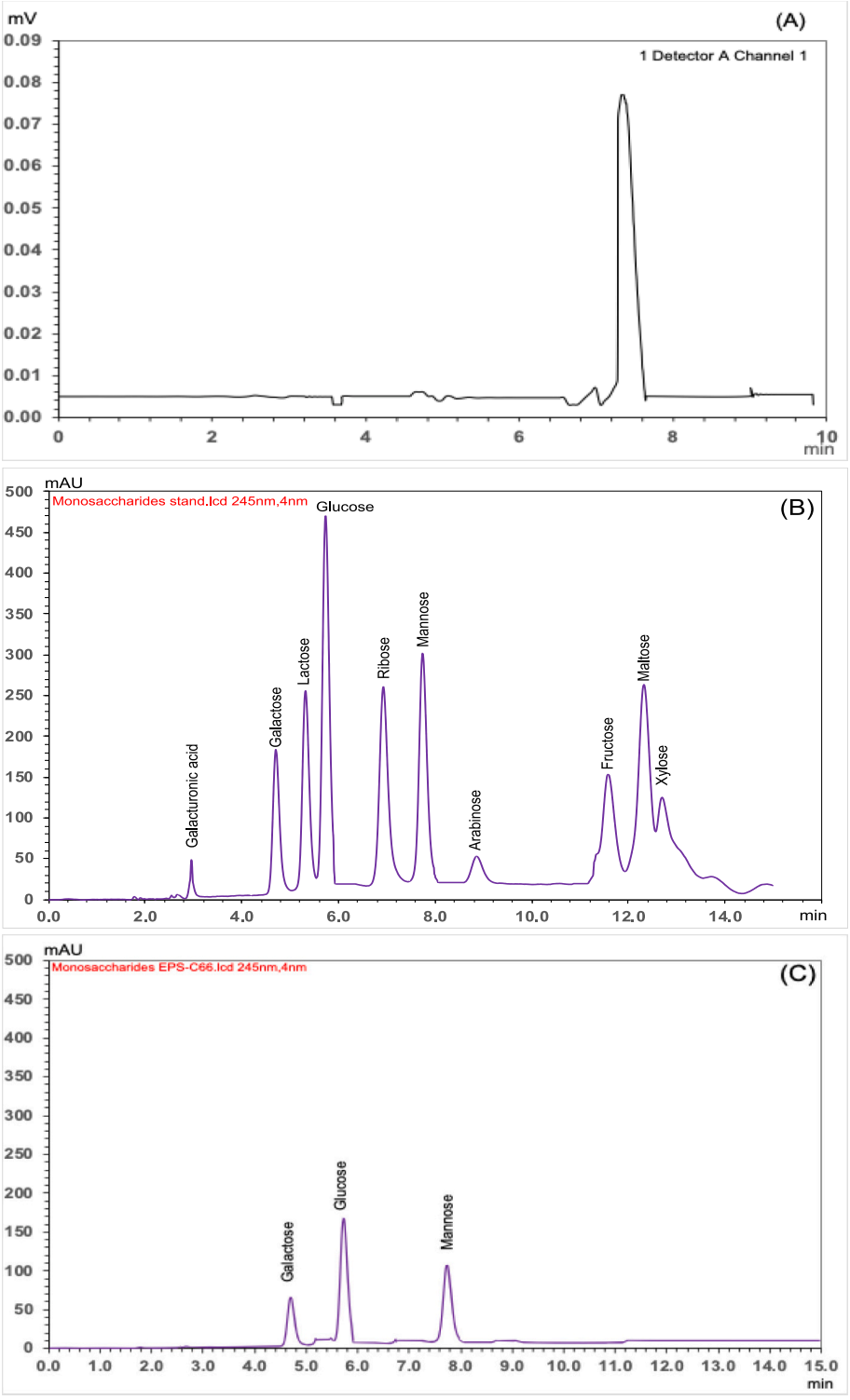

Fig. 1. Molecular weight (A), monosaccharides standard (B), and EPC-C66 monosaccharide composition.

of the EPS (Zhou et al., 2019). Our results differ from the monosaccharide composition of EPS produced by L. *reuteri* DSM 17938 (Kšonžeková et al., 2016) and *L. reuteri* SK24.003 (Miao et al., 2015) who reported only one monosaccharide type (glucose) as a composition. This indicates that the current EPS-C66 possesses different functionalities compared to those previously reported.

3.2. FT-IR and NMR analysis

FT-IR functional group analysis is shown in Fig. 2. The presence of the α- and β-configurations of monosaccharides was indicated by peaks at 529.9 cm^{-1} and 814.6 cm^{-1}. The FT-IR spectra revealed various peak positions: the stretching vibration of CH formed a peak at 2926.1 cm^{-1}, while the broad stretching vibration at 3299.2 cm^{-1} indicated hydroxyl groups. Additionally, the pyranose ring vibration demonstrated a distinct peak at 1213.8 cm^{-1}, and the presence of monosaccharides generated a peak at 917.1 cm^{-1}. The current FITR spectrum is comparable to the FTIR spectrum of EPS produced by *L. reuteri* E81 (İspirli et al., 2019). The difference is mainly due to the monosaccharide composition between the EPS-C66 and EPS-E81.

Concerning NMR analysis, the ^{1}H, ^{13}C, $^{1}H—^{1}H$ TOCSY, $^{13}C—^{1}H$ HQSC, and $^{13}C—^{1}H$ HMBC NMR spectra are shown in Fig. 3A, B, C, D, and E, respectively. The ^{1}H peaks between 3 and 4 ppm were assigned to the protons of C2–C6 (Ye et al., 2018). The anomeric region appeared at chemical shifts in the range of 4.5–5.5 ppm. The occurrence of peaks at 172.7, 176.5, and 177.1 ppm in ^{13}C NMR spectra (Fig. 3B) and the observation of a strong HSQC correlation linking a carbon at 76.8 ppm to a proton at 5.37 ppm, accompanied by a weaker one at 72.6 and 4.62 ppm (Fig. 3C), could be considered the signature of the presence of uronic acid functions in EPS-3, in either α- and β-anomeric configuration (Ma et al., 2018). The $^{1}H—^{13}C$ NMR HQSC spectrum (Fig. 3C) displayed seven major anomeric correlation signals, which may be ascribed to α/β links of D-glucopyranose, D-mannopyranose, and D-galactopyranose (Zhou et al., 2019). The current NMR spectra differ from those reported by Kšonžeková et al. (2016) for EPS produced by L. *reuteri* DSM 17938. This suggests that the EPS structure is strain-dependent. The EPS structures produced by the current strain and L. *reuteri* DSM 17938 are different. The CASPER computed assignments (Lundborg & Widmalm, 2011) of the experimental anomeric CH correlations obtained from $^{1}H—^{13}C$ NMR HQSC are presented in Table 1. Based on the results from CASPER, the suggested backbone structure of EPS-3 was →4)α-d-Man(1 → 4)α-d-Glc(1 → 4)β-d-Gal(1 → 6)β-d-Man(1 → 3)β-d-Glc(1 → 6)α-d-Glc (1 → 2)β-d-Glc(1 → 6)α-d-Gal(1 → .

3.3. SEM, thermal properties, zeta potential, and particle size

3.3.1. SEM and thermal properties

Scanning electron microscopy (SEM) has become recognized as an effective technique for examining the surface morphology of polysaccharides (Zhao et al., 2021). SEM images at 800× (Fig. 4A) and 1800× (Fig. 4B) magnifications of EPS-C66 revealed a layer-like, flake-like, and compact structure. The layer-like structure provides firm structural qualities that may be caused by the presence of α- and β-linkages (Zhou et al., 2019). Additionally, the SEM scan showed that EPS-C66 had a porous structure. The porous network potentially facilitates the retention of excess moisture, which is an advantageous feature for food production, such as cheesemaking (Bamigbade et al., 2023) and fermented milk.

The thermodynamic curves are indicated in Fig. 4C. The transition temperature (T_g) of EPS-C66 was found to be 50.03 °C. A prominent peak indicating the melting temperature was found to be at 161.08 °C. At the T_m, the enthalpy energy was 204.00 J/g. EPS-C66's current Tm is higher than EPS generated by L. *reuteri* SK24.003 (T_m 147.7 °C) (Miao et al., 2015) and *L. plantarum* BR2 (Tm 97.3 °C) (Sasikumar et al., 2017). However, T_m of EPS-C66 is lower than EPS produced by L. *reuteri* E81, which has a T_m of 290 °C (İspirli et al., 2019). The higher T_m values indicated that EPS-C66 was stable at higher temperatures, which is advantageous for thermal processing in the food and dairy manufacturing industries.

3.3.2. Zeta potential and particle size

The particle size analyzer determined that the average size and zeta

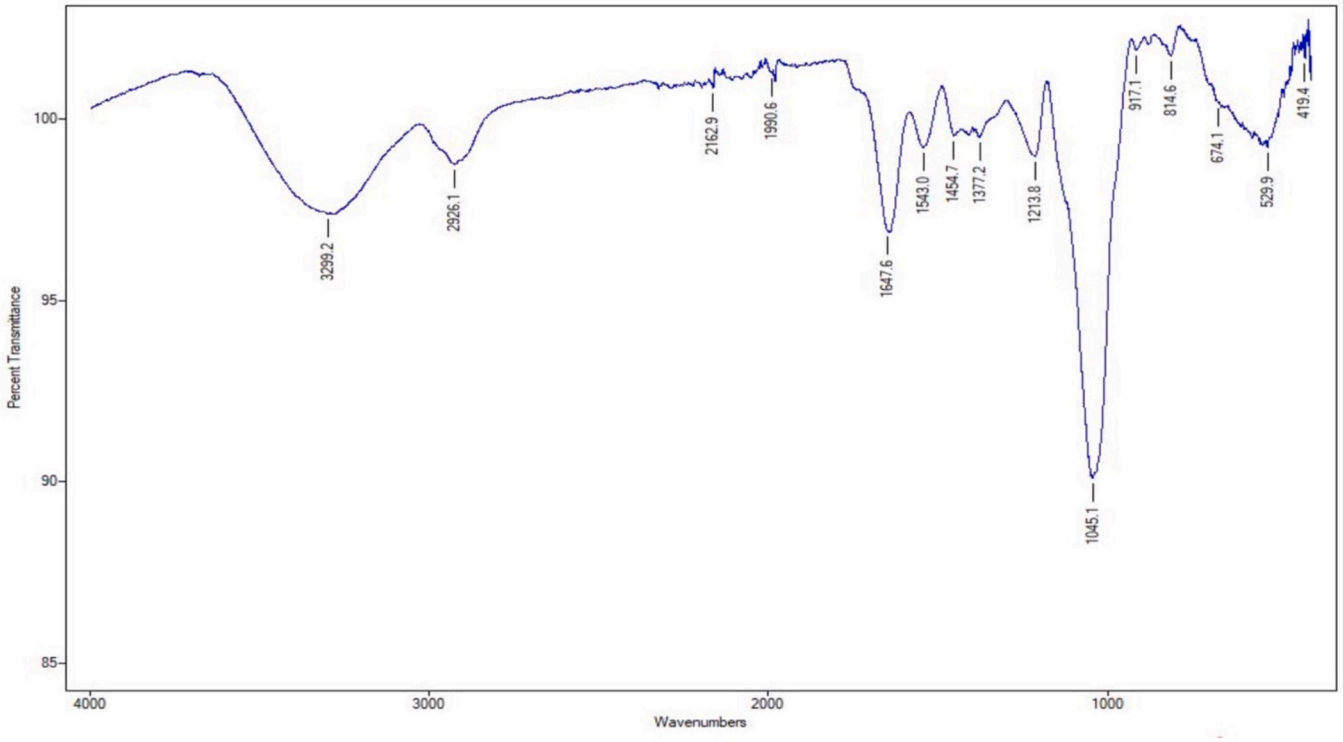

Fig. 2. FTIR spectrum of EPS-C66.

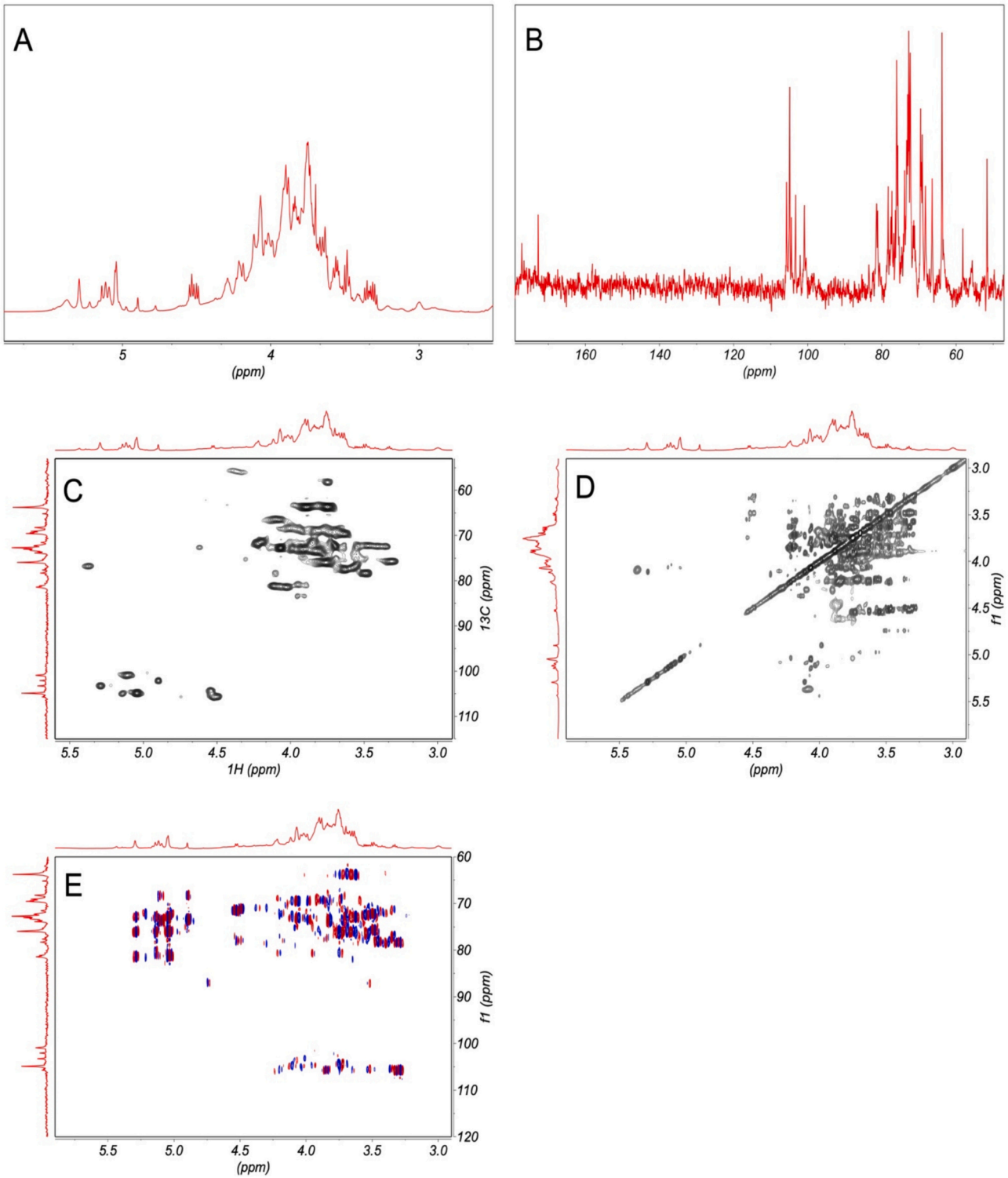

Fig. 3. 1D and 2D NMR analysis of EPS-C66. A) Region from 1D ^{1}H spectrum. B) Region from 1D ^{13}C spectrum. C) Region from 2D ^{1}H TOCSY. D) Region from 2D ^{13}C—^{1}H HSQC spectrum. E) Overlay of 2D ^{13}C—^{1}H HSQC (black contours) and 2D ^{13}C—^{1}H HMBC (red-blue contours). (For interpretation of the references to colour in this figure legend, the reader is referred to the web version of this article.)

potential of EPS-C66 were 1510.4 nm and − 314.5 mV, respectively. The size and charge of EPS-C66 are comparable to those reported for EPS produced by *Pediococcus pentosaceus* M41 (Ayyash, Abu-Jdayil, Olaimat, et al., 2020). Negative charge is typically associated with notable bioactive properties of EPS (Xu et al., 2019b). The negative charge of EPS-C66 may be attributed to hydroxyl and carboxyl groups present in the EPS structure.

3.4. Bioactive properties

3.4.1. Antioxidant capacity

At a concentration of 5 mg/mL, EPS-C66 demonstrated radical scavenging activities of 42.7 % and 27.1 % in the DPPH and ABTS assays, respectively. When the concentration was increased to 10 mg/mL, the radical scavenging activity significantly ($P < 0.05$) increased to

Table 1
Chemical shifts assignments of NMR spectra.

Residues	Chemical shifts (ppm)					
	1	2	3	4	5	6,6'
→6)α-d-Gal^{i}(1→	102.67	69.44	69.44	69.44	71.64	69.44
	5.29	3.83	3.83	3.83	4.79	3.65,3.83
→2)β-d-Glc^{ii}(1→	104.86	79.75	75.92	n.d.	77.47	61.91
	5.04	3.49	3.76	n.d.	3.63	3.73,3.93
→6)α-d-Glc^{iii}(1→	100.91	72.23	73.06	69.44	71.64	68.78
	5.11	3.47	3.83	3.65	4.72	3.94,4.52
→3)β-d-Glc^{iv}(1→	104.65	72.81	82.45	69.44	76.52	61.87
	4.99	3.55	4.03	3.65	3.32	3.74,3.92
→6)β-d-Man^{v}(1→	102.13	71.64	72.81	66.50	76.54	68.22
	5.18	4.69	3.55	4.09	3.56	4.00,5.39
→4)β-d-Gal^{vi}(1→	105.57	72.30	73.00	81.31	76.74	61.15
	4.96	3.70	3.91	4.11	4.08	4.98,5.01
→4)α-d-Glc^{vii}(1→	102.90	72.81	75.53	79.54	72.63	61.49
	5.14	3.55	4.31	3.95	4.89	3.78,3.81
→4)α-d-Man^{viii}(1→	103.25	71.64	72.73	77.96	73.06	63.74
	5.22	4.21	4.07	4.10	3.83	3.75,4.99

67.9 % in the DPPH assay and 31.3 % in the ABTS assay (Table 2). These results are consistent with those obtained in previous studies (Amiri et al., 2019; Ayyash, Abu-Jdayil, Olaimat, et al., 2020). The concentration and structure of the produced EPS may contribute to their antioxidant capacity. Certain structural features, such as the presence of functional groups or molecular weight, can influence their ability to scavenge free radicals and protect against oxidative stress (Zhou et al., 2019).

3.4.2. Antidiabetic activity

Inhibition of α-amylase is an indirect approach to controlling diabetes by reducing sugar intake from carbohydrate/starch hydrolysis. EPS-C66 showed potent inhibitory activities against α-amylase (87.1 %) and α-glucosidase (87.2 %) at 100 μg/mL, and 88.4 % and 88.2 %, respectively, at 200 μg/mL (Table 2). The values of antidiabetic activity obtained in the present study are comparable to those reported in another study (Ayyash, Abu-Jdayil, Itsaranuwat, et al., 2020), except for the α-amylase value (88.4 %) at 200 μg/mL. Comparatively, the inhibitory rate of α-amylase was found to be 90.6 % for L. *acidophilus* (Raj et al., 2024), which was higher than that in the present study. However, the inhibitory rate of α-glucosidase was 68.7 % for *L. acidophilus* (Raj et al., 2024), which were lower than that in the present study (Raj et al., 2024). Additionally, it was observed that the α-glucosidase inhibition rate of LAB strains ranged from 19.8 % to 72.3 % (Jeong et al., 2021). The α-glucosidase inhibition rates of L. *gasseri* MG4524, *L. rhamnosus* MG4502, and L. *reuteri* MG5149 were found to be 63.8 %, 63.4 %, and 60.3 %, respectively (Jeong et al., 2021), which were lower than our findings. The glycosidic linkages in EPS might have the ability to inhibit the activity of both α-amylase and α-glucosidase enzymes (Robyt, 2005). *L. rhamnosus* GG (LGG), one of the most well-studied probiotic LAB, significantly decreased blood glucose levels and improved hyperglycemia in neonatal streptozotocin-induced diabetic rats, thus proving its antidiabetic potential (Jeong et al., 2021).

The inhibitory impact of EPS on α-amylase and α-glucosidase may stem from competitive and non-competitive interactions between EPS and the enzymes' active or allosteric sites. EPS can also function as a physical barrier or engage directly with enzymes, hindering substrate access. Additionally, the functional groups in EPS, such as hydroxyl and carboxyl groups, might establish hydrogen bonds or ionic interactions with essential residues in the enzyme active sites, which further boosts their inhibitory potential (Zhang et al., 2023). These findings suggest that EPS-C66 could directly influence glucose metabolism. Moreover, it might impact the composition and activity of the gut microbiota. A balanced gut microbiota has been associated with improved metabolic health, including better glucose regulation and insulin sensitivity, which are key factors in managing diabetes.

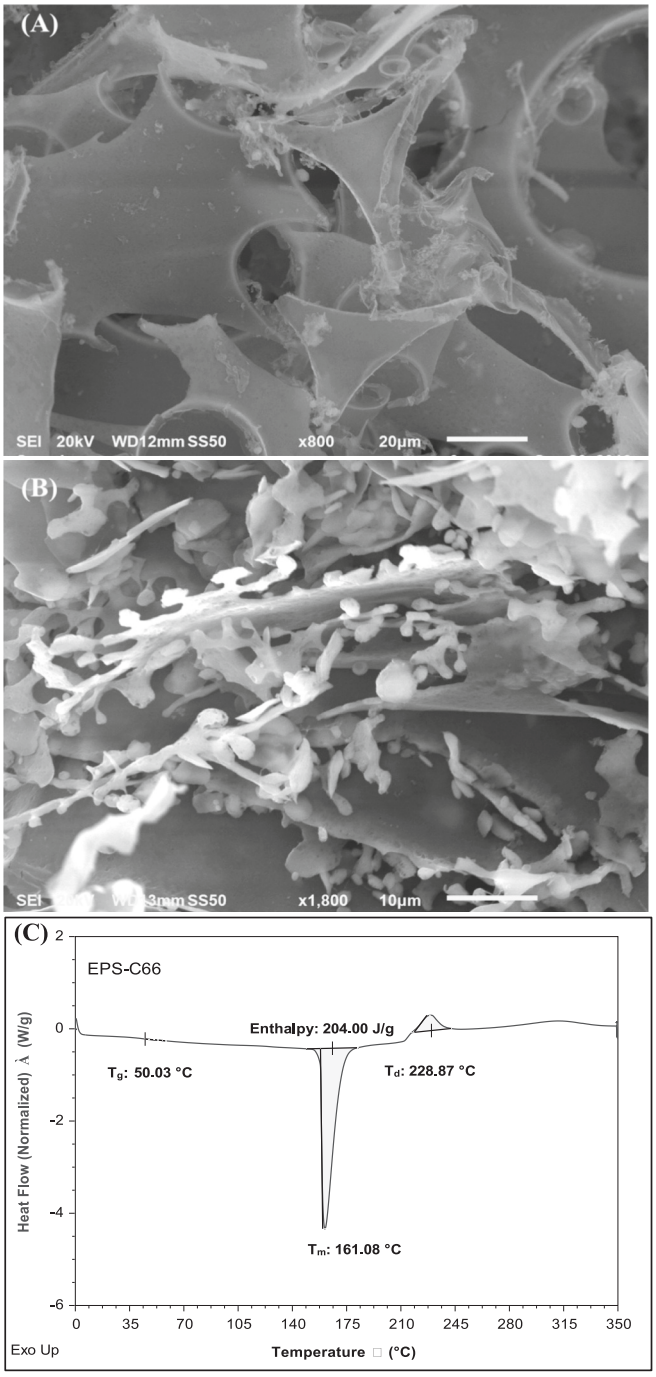

Fig. 4. SEM images at magnifications 800× (A) and 1800× (B) and DSC thermogram (C) of EPS-C66.

3.4.3. Antibacterial activity

The antibacterial activity of EPS-C66 was assessed against four prevalent foodborne pathogens. Table 2 demonstrates the remarkable antibacterial activity of EPS-C66, with pathogen population reductions ranging from 2.89 log to 3.27 log CFU/mL. EPS-C66 can achieve an approximate decrease of 3.0 logs, which is advantageous considering the high initial bacterial load (9 logs). This indicates that EPS-C66 can effectively inhibit or even kill pathogens. There was no significant difference in log reduction among the four pathogens (Table 2). Our results are similar to those obtained previously (Ayyash, Abu-Jdayil, Olaimat, et al., 2020), except for *S. aureus* and *S. typhimurium*. The formation of an antibiofilm by EPS has been observed in some studies (Liu et al., 2017; Wang et al., 2015), but the effectiveness of the drug for this purpose

Table 2
Bioactivities of EPS-C66: antioxidant capacity (5 mg and 10 mg), antidiabetic (100 μg and 200 μg), anticancer activities (5 mg and 10 mg) and antipathogenic activity (5 mg/mL). Values are mean ± standard error of triplicates.

Attributes	EPS-C66 concentration	
Antioxidant capacity	5 mg/mL	10 mg/mL
DPPH (%)	42.7 ± 2.73^{aB}	67.9 ± 7.69^{aA}
ABTS (%)	27.1 ± 1.28^{bB}	31.3 ± 1.28^{aA}
Antidiabetic activities	100 μg /mL	200 μg /mL
Amylase inhibition (%)	87.1 ± 1.51^{aA}	88.4 ± 1.85^{aA}
Glucosidase inhibition (%)	87.2 ± 0.53^{aA}	88.2 ± 0.22^{aA}
Anticancer activities	5 mg/mL	10 mg/mL
Caco-2	88.9 ± 14.22^{aA}	93.7 ± 8.32^{aA}
MCF-7	32.0 ± 0.61^{bB}	61.4 ± 11.32^{bA}
Antipathogenic activities	Log CFU/mL	Reduction
Staphylococcus aureus	5.9 ± 0.49	3.13
Salmonella Typhimurium	6.1 ± 0.17	2.89
Listeria monocytogenes	6.0 ± 0.24	2.98
E. coli O157:H7	5.7 ± 0.45	3.27

remains uncertain (Wang et al., 2015). Several factors could be responsible for the remarkable antibacterial activity of EPS-C66, such as: (i) EPS-C66 might interfere with biofilm formation or destabilize existing biofilms, making bacteria more susceptible to immune clearance or antibiotic treatment. (ii) The observed antibacterial action of generated EPS-C66 may be partially explained by the disruption of bacterial cell membranes, which allows for the loss of cellular contents, as well as the suppression of vital bacterial enzymes involved in activities like DNA replication and protein synthesis (Jeong et al., 2017; Xu et al., 2019b).

3.4.4. Anticancer activity

The colon (Caco-2) and breast (MCF-7) cancer cell lines were significantly inhibited by EPS-C66, as shown in Table 2. EPS-C66 demonstrated an antitumor inhibition rate of 88.9 % and 32.0 % at 5 mg/mL, against Caco-2 and MCF-7, respectively. EPS-C66 showed a significant increase ($P < 0.05$) in its ability to inhibit tumors at 10 mg/mL to 93.7 % and 61.4 % for Caco-2 and MCF-7 cells, respectively. The level of inhibition of Caco-2 cells in this study is similar to that observed for EPS produced by *R. mucilaginosa* CICC (Ma et al., 2018). The antitumor properties of EPS-C66 have been found to be particularly effective against colon cancer cells (Caco-2) and breast cancer (MCF-7) cells (Table 2). The anticancer activities of L. *acidophilus* LA-EPS-20079 against both Caco-2 and MCF-7 cells reached 80.65 % and 71.86 %, respectively, at 10 mg/mL in cellular proliferation (BRDU cellular incorporation), being significantly different from the non-treated cells (El-Deeb et al., 2018). The specific mechanism(s) behind EPS's anticancer effects is not entirely clear. Several potential reasons exist for the anticancer effects of EPS-C66, including the promotion of apoptosis in cancer cells and competition with growth factors like tumor necrosis factor at cell receptors. Additionally, EPS may stimulate autophagy by influencing the Beclin-I protein. It might also inhibit cancer cell receptors, thereby preventing growth promoters from accessing the cells (Kim et al., 2010).

3.5. Rheological behaviours

3.5.1. Apparent viscosity and flow curves of EPS-C66

The EPS-C66 solutions showed a decrease in apparent viscosity (η) as the shear rate increased from 0 to 1000 s^{-1} (Fig. 5A). The apparent viscosity of EPS-C66 solutions decreased when NaCl or $CaCl_2$ was added. This implies that the behavior of EPS-C66 is non-Newtonian (shear-thinning). The electrolyte's screening effect on intermolecular hydrogen bonding could be responsible for the decrease in EPS-C66 viscosity and may also result in a decrease in the strength of the three-dimensional network (Abid et al., 2021). This result is consistent with EPS generated by *Mesorhizobium loti* (de Oliveira et al., 2018). Furthermore, by curling polymer coils, the intramolecular electrostatic repulsions

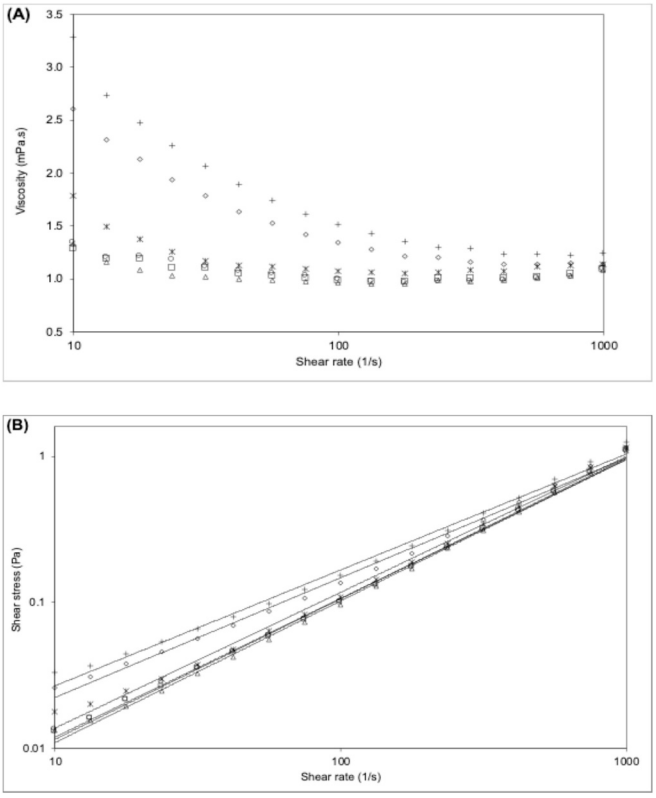

Fig. 5. Apparent viscosity (A) and flow curves fitted with power law mode (B) of EPS-C66 in $CaCl_2$ pH 6.0 (◇), $CaCl_2$ pH 4.0 (□), NaCl pH 6.0 (○), NaCl pH 4.0 (△), H_2O pH 6.0 (+), H_2O pH 4.0 (×).

between the negatively charged groups in EPS-C15 molecules can reduce this viscosity (Abid et al., 2021).

When shear rates were below 100 s^{-1}, the impact of pH was more noticeable than that of salt types. Specifically, EPS solutions with a pH of 6.0 displayed a higher viscosity than those with an adjusted pH of 4.0 (Fig. 5A). This suggests that the type of salt did not affect the apparent viscosity, which is explained by the fact that the ionization degree of carboxyl groups in polysaccharide molecules increased as the pH value increased (Bamigbade et al., 2023). However, in a different investigation, the presence of $CaCl_2$ was found to increase the viscosity of EPS generated by *Sporidiobolus pararoseus* JD-2 (Han et al., 2016). These variations across studies could be attributed to differences in the molecular weight (Mw) and monosaccharide composition of EPS produced by microbes of different genera, species, and strains. Overall, EPS-C66 demonstrated stability when exposed to monovalent ions (Na^+) (Fig. 5A). The Power law model fits the flow curves well ($R^2 > 0.99$) (Fig. 5B; Table S1).

The rheological properties of EPS-C66 solutions, which display shear-thinning behavior, are highly relevant to food systems, particularly in areas such as food texture, yogurt viscosity, and creaminess. The reduction in apparent viscosity as shear rate increases and the presence of electrolytes like NaCl and CaCl2 indicate that the viscosity modulation by EPS-C66 is shaped by its molecular interactions, encompassing electrostatic repulsions and the disruption of hydrogen bonds. The pH-dependent behavior of viscosity, with notable increases at pH 6.0, implies that EPS-C66 could improve the creaminess and mouthfeel of products like yogurt, where consistent viscosity and texture are essential.

3.5.2. Amplitude and frequency sweeps

The amplitude sweep curves for G' and G" of EPS-C66, displayed in Fig. S1, show a general decrease in modulus with increasing strain across

different pH levels and ionic conditions. Both moduli G' and G" are highest in $CaCl_2$ at pH 4.0 and lowest in H_2O at pH 4.0, indicating that ionic strength and pH significantly influence the mechanical properties of EPS-C66 (Fig. S1).

The frequency sweep curves for G' and G" of EPS-C66 indicate that both the storage modulus (G') and loss modulus (G") increase with frequency across all conditions (Fig. S2). The highest values for both moduli are observed in $CaCl_2$ at pH 4.0, suggesting that the ionic environment and lower pH enhance the viscoelastic properties of EPS-C66. Conversely, the lowest values are seen in H_2O at pH 4.0, highlighting the significant role of ionic strength in modulating the mechanical behavior. These results demonstrate that the viscoelastic properties of EPS-C66 are highly dependent on the ionic composition and pH of the surrounding medium, with calcium ions providing the most substantial reinforcement effect (Fig. S2). Tan delta (δ) of EPS-C66 shows a decrease with increasing frequency across all conditions (Fig. S3). Higher tan delta values, indicating more liquid-like behavior, are seen in H_2O at both pH levels. Lower values, indicating more solid-like behavior, are observed in $CaCl_2$, particularly at pH 4.0, highlighting the strong influence of calcium ions and acidic conditions in enhancing the elastic nature of EPS-C66. The higher storage modulus (G') and loss modulus (G") observed with CaCl2 at pH 4.0 indicate that the presence of calcium ions improves the rigidity and stability of the exopolysaccharide, making it more suitable for applications in food systems where texture and stability are key. Additionally, the reduced tan delta values in CaCl2 at pH 4.0, which suggest a more solid-like consistency, mean that EPS-C66 is particularly effective for enhancing the texture of food items like yogurt and dressings by boosting creaminess, stability, and viscosity. These characteristics can aid in stabilizing emulsions, enhancing mouthfeel, and ensuring consistency, especially in products that demand a smooth and uniform texture, showcasing EPS-C66's potential as a natural stabilizer and texturizer in the food industry.

3.5.3. *Temperature-dependent behavior*

The apparent viscosity as a function of temperature is displayed in Fig. 6, illustrating how all EPS-C66 solutions behaved differently depending on temperature. With rising temperatures, viscosities of all EPS-C66 solutions decreased (Fig. 6). Significant activation was seen in the EPS-C66 solution containing $CaCl_2$ at pH 6.0 (Table S1). This is consistent with EPS-C66's apparent viscosity. The temperature-dependent behavior was significantly influenced by the pH value (6.0) and salt type (Ca^{2+}). This could be explained by the formation of intermolecular cross-linkage bridges by Ca^{2+} at pH 6.0. We hypothesize that the intermolecular linkage bridges formed by Ca^{2+} were not supported by pH 4.0. The temperature-dependent behavior of EPS-C66 in the presence of monovalent Na^{+} was demonstrated to be stable in Fig. 6. The differences in apparent viscosities between the EPS-C66 solutions decreased until 80 °C after 55 °C. This result implies that high-heat processes are unsuitable for the current EPS-C66. This outcome is consistent with the temperature-dependent behaviours of EPS-JD2 (Han et al., 2016).

4. Conclusion

EPS are valuable biopolymers with a wide range of potential applications in pharmaceuticals, food ingredients, adhesives, textiles, and cosmetics. Due to its significant bioactive properties and relatively high molecular weight, EPS-C66 is a promising candidate as a functional ingredient that can be used in various food formulations. All EPS-C66 samples exhibited shear-thinning characteristics. The rheological properties were influenced by pH level and salt content. EPS-C66 produced by L. *reuteri* C66 has the potential to enhance the appearance, rheological properties, texture, and mouthfeel of fermented dairy products such as yogurt. Consequently, EPS-C66 is considered an attractive ingredient in the food industry, potentially serving as a viscosifier, stabilizer, emulsifying agent, or gelling agent.

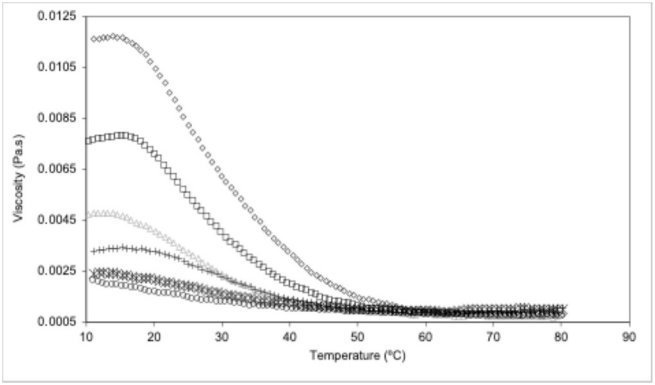

Fig. 6. Temperature-dependent behavior of EPS-C66 in $CaCl_2$ pH 6.0 (◇), $CaCl_2$ pH 4.0 (□), NaCl pH 6.0 (○), NaCl pH 4.0 (△), H_2O pH 6.0 (+), H_2O pH 4.0 (×).

CRediT authorship contribution statement

A.K.M. Humayun Kober: Writing – original draft, Formal analysis. **Mohamed Abdin:** Writing – original draft, Formal analysis. **Athira Subhash:** Writing – review & editing, Investigation. **Shao-Quan Liu:** Writing – review & editing, Validation. **Enes Dertli:** Writing – review & editing, Validation. **Basim Abu-Jdayil:** Writing – review & editing, Investigation. **Pau-Loke Show:** Writing – review & editing, Validation. **Mutamed Ayyash:** Writing – review & editing, Visualization, Validation, Supervision, Resources, Project administration, Funding acquisition, Formal analysis, Data curation, Conceptualization.

Declaration of competing interest

The authors declare that they have no known competing financial interests or personal relationships that could have appeared to influence the work reported in this paper.

Acknowledgment

The authors thank the United Arab Emirates University (UAEU) for funding this project *via* grant number 12R105.

Appendix A. Supplementary data

Supplementary data to this article can be found online at https://doi.org/10.1016/j.fochx.2025.102164.

Data availability

Data will be made available on request.

References

Abid, Y., Azabou, S., Blecker, C., Gharsallaoui, A., Corsaro, M. M., Besbes, S., & Attia, H. (2021). Rheological and emulsifying properties of an exopolysaccharide produced by potential probiotic Leuconostoc citreum-BMS strain. *Carbohydrate Polymers, 256*, Article 117523. https://doi.org/10.1016/j.carbpol.2020.117523

Abushelaibi, A., Al-Mahadin, S., El-Tarabily, K., Shah, N. P., & Ayyash, M. (2017). Characterization of potential probiotic lactic acid bacteria isolated from camel milk [article]. *LWT, 79*, 316–325. https://doi.org/10.1016/j.lwt.2017.01.041

Amiri, S., Rezaei Mokarram, R., Sowti Khiabani, M., Rezazadeh Bari, M., & Alizadeh Khaledabad, M. (2019). Exopolysaccharides production by Lactobacillus acidophilus LA5 and Bifidobacterium animalis subsp. lactis BB12: Optimization of fermentation variables and characterization of structure and bioactivities. *International Journal of Biological Macromolecules, 123*, 752–765. https://doi.org/10.1016/j.ijbiomac.2018.11.084

Ayyash, M., Abu-Jdayil, B., Itsaranuwat, P., Galiwango, E., Tamiello-Rosa, C., Abdullah, H., … Hamed, F. (2020). Characterization, bioactivities, and rheological properties of exopolysaccharide produced by novel probiotic Lactobacillus

plantarum C70 isolated from camel milk. *International Journal of Biological Macromolecules, 144*, 938–946. https://doi.org/10.1016/j.ijbiomac.2019.09.171

Ayyash, M., Abu-Jdayil, B., Olaimat, A., Esposito, G., Itsaranuwat, P., Osaili, T., … Liu, S. Q. (2020). Physicochemical, bioactive and rheological properties of an exopolysaccharide produced by a probiotic Pediococcus pentosaceus M41. *Carbohydrate Polymers, 229*, Article 115462. https://doi.org/10.1016/j.carbpol.2019.115462

Bakry, I. A., Yang, L., Farag, M. A., Korma, S. A., Khalifa, I., Cacciotti, I., … Wei, W. (2021). A comprehensive review of the composition, nutritional value, and functional properties of camel milk fat. *Foods, 10*(9), 2158.

Bamigbade, G., Ali, A. H., Subhash, A., Tamiello-Rosa, C., Al Qudsi, F. R., Esposito, G., … Ayyash, M. (2023). Structural characterization, biofunctionality, and environmental factors impacting rheological properties of exopolysaccharide produced by probiotic Lactococcus lactis C15. *Scientific Reports, 13*(1), 17888. https://doi.org/10.1038/s41598-023-44728-w

Bamigbade, G. B., Subhash, A. J., Al-Ramadi, B., Kamal-Eldin, A., Gan, R. Y., Liu, S. Q., & Ayyash, M. (2024). Gut microbiota modulation, prebiotic and bioactive characteristics of date pomace polysaccharides extracted by microwave-assisted deep eutectic solvent [article]. *International Journal of Biological Macromolecules, 262, Article 130167*. https://doi.org/10.1016/j.ijbiomac.2024.130167

Bubb, W. A. (2003). NMR spectroscopy in the study of carbohydrates: Characterizing the structural complexity. *Concepts in Magnetic Resonance Part A, 19a(1)*, 1–19. https://doi.org/10.1002/cmr.a.10080

El-Deeb, N. M., Yassin, A. M., Al-Madboly, L. A., & El-Hawiet, A. (2018). A novel purified exopolysaccharide, LA-EPS-20079, molecularly regulates both apoptotic and NF-κB inflammatory pathways in human colon cancer. *Microbial Cell Factories, 17*, 1–15. https://doi.org/10.1186/s12934-018-0877-z

Han, M., Du, C., Xu, Z. Y., Qian, H., & Zhang, W. G. (2016). Rheological properties of phosphorylated exopolysaccharide produced by Sporidiobolus pararoseus JD-2. *International Journal of Biological Macromolecules, 88*, 603–613. https://doi.org/10.1016/j.ijbiomac.2016.04.035

İspirli, H., Sagdic, O., Yılmaz, M. T., & Dertli, E. (2019). Physicochemical characterisation of an α-glucan from Lactobacillus reuteri E81 as a potential exopolysaccharide suitable for food applications. *Process Biochemistry, 79*, 91–96. https://doi.org/10.1016/j.procbio.2018.12.015

Jeong, D., Kim, D. H., Kang, I. B., Kim, H., Song, K. Y., Kim, H. S., & Seo, K. H. (2017). Characterization and antibacterial activity of a novel exopolysaccharide produced by DN1 isolated from kefir. *Food Control, 78*, 436–442. https://doi.org/10.1016/j.foodcont.2017.02.033

Jeong, Y., Kim, H., Lee, J. Y., Won, G., Choi, S. I., Kim, G. H., & Kang, C. H. (2021). The antioxidant, anti-diabetic, and anti-Adipogenesis potential and probiotic properties of lactic acid Bacteria isolated from human and fermented foods. *Fermentation, 7*(3), 123. https://doi.org/10.3390/fermentation7030123

Kim, Y., Oh, S., Yun, H., Oh, S., & Kim, S. (2010). Cell-bound exopolysaccharide from probiotic bacteria induces autophagic cell death of tumour cells. *Letters in Applied Microbiology, 51*(2), 123–130. https://doi.org/10.1111/j.1472-765X.2010.02859.x

Kober, A. K. M. H., Saha, S., Ayyash, M., Namai, F., Nishiyama, K., Yoda, K., … Kitazawa, H. (2024). Insights into the anti-Adipogenic and anti-inflammatory potentialities of probiotics against obesity. *Nutrients, 16*(9), 1373. https://doi.org/10.3390/nu16091373

Kšonžeková, P., Bystrický, P., Vlčková, S., Pätoprstý, V., Pulzová, L., Mudroňová, D., … Tkáčiková, Ľ. (2016). Exopolysaccharides of Lactobacillus reuteri: Their influence on adherence of E. Coli to epithelial cells and inflammatory response. *Carbohydrate Polymers, 141*, 10–19. https://doi.org/10.1016/j.carbpol.2015.12.037

Liu, Z., Zhang, Z., Qiu, L., Zhang, F., Xu, X., Wei, H., & Tao, X. (2017). Characterization and bioactivities of the exopolysaccharide from a probiotic strain of Lactobacillus plantarum WLPL04. *Journal of Dairy Science, 100*(9), 6895–6905. https://doi.org/10.3168/jds.2016-11944

Lundborg, M., & Widmalm, G. (2011). Structural analysis of glycans by NMR chemical shift prediction. *Analytical Chemistry, 83*(5), 1514–1517. https://doi.org/10.1021/ac1032534

Ma, W., Chen, X., Wang, B., Lou, W., Chen, X., Hua, J., … Peng, T. (2018). Characterization, antioxidativity, and anti-carcinoma activity of exopolysaccharide extract from Rhodotorula mucilaginosa CICC 33013. *Carbohydrate Polymers, 181*, 768–777. https://doi.org/10.1016/j.carbpol.2017.11.080

Miao, M., Ma, Y., Huang, C., Jiang, B., Cui, S. W., & Zhang, T. (2015). Physicochemical properties of a water soluble extracellular homopolysaccharide from Lactobacillus reuteri SK24.003. *Carbohydrate Polymers, 131*, 377–383. https://doi.org/10.1016/j.carbpol.2015.05.066

Nabot, M., Guerin, M., Sivakumar, D., Remize, F., & Garcia, C. (2022). Variability of bacterial Homopolysaccharide production and properties during food processing. *Biology (Basel), 11*(2), 171. https://doi.org/10.3390/biology11020171

de Oliveira, J. M., Amaral, S. A., & Burkert, C. A. V. (2018). Rheological, textural and emulsifying properties of an exopolysaccharide produced by Mesorhizobium loti grown on a crude glycerol-based medium. *International Journal of Biological Macromolecules, 120*, 2180–2187. https://doi.org/10.1016/j.ijbiomac.2018.06.158

Raj, S. T., Puspanadan, S., Gan, C. Y., & Tan, J. S. (2024). Purification of exopolysaccharide produced from Lactobacillus spp. using ionic-liquid as adjuvant in alcohol/salt-based aqueous two-phase system for its antidiabetic properties. *International Journal of Biological Macromolecules, 267*, Article 131376. https://doi.org/10.1016/j.ijbiomac.2024.131376

Robyt, J. F. (2005). Inhibition, activation, and stabilization of α-amylase family enzymes. *Biologia (Lahore, Pakistan), 60*(16), 17–26. ://WOS:000234899500004.

Saadat, Y. R., Khosroushahi, A. Y., & Gargari, B. P. (2019). A comprehensive review of anticancer, immunomodulatory and health beneficial effects of the lactic acid bacteria exopolysaccharides. *Carbohydrate Polymers, 217*, 79–89. https://doi.org/10.1016/j.carbpol.2019.04.025

Sasikumar, K., Kozhummal Vaikkath, D., Devendra, L., & Nampoothiri, K. M. (2017). An exopolysaccharide (EPS) from a Lactobacillus plantarum BR2 with potential benefits for making functional foods. *Bioresource Technology, 241*, 1152–1156. https://doi.org/10.1016/j.biortech.2017.05.075

Sørensen, H. M., Rochfort, K. D., Maye, S., MacLeod, G., Brabazon, D., Loscher, C., & Freeland, B. (2022). Exopolysaccharides of lactic acid bacteria: Production, purification and health benefits towards functional food. *Nutrients, 14*(14), 2938. https://doi.org/10.3390/nu14142938

Wang, J., Zhao, X., Yang, Y., Zhao, A., & Yang, Z. (2015). Characterization and bioactivities of an exopolysaccharide produced by Lactobacillus plantarum YW32. *International Journal of Biological Macromolecules, 74*, 119–126. https://doi.org/10.1016/j.ijbiomac.2014.12.006

Wu, J., Han, X., Ye, M., Li, Y., Wang, X., & Zhong, Q. (2023). Exopolysaccharides synthesized by lactic acid bacteria: Biosynthesis pathway, structure-function relationship, structural modification and applicability. *Critical Reviews in Food Science and Nutrition, 63*(24), 7043–7064.

Xu, Y., Cui, Y., Yue, F., Liu, L., Shan, Y., Liu, B., Zhou, Y., & Lü, X. (2019a). Exopolysaccharides produced by lactic acid bacteria and Bifidobacteria: Structures, physiochemical functions and applications in the food industry. *Food Hydrocolloids, 94*, 475–499.

Xu, Y. M., Cui, Y. L., Yue, F. F., Liu, L. H., Shan, Y. Y., Liu, B. F., … Lü, X. (2019b). Exopolysaccharides produced by lactic acid bacteria and Bifidobacteria: Structures, physiochemical functions and applications in the food industry. *Food Hydrocolloids, 94*, 475–499. https://doi.org/10.1016/j.foodhyd.2019.03.032

Ye, G., Chen, Y., Wang, C., Yang, R., & Bin, X. (2018). Purification and characterization of exopolysaccharide produced by Weissella cibaria YB-1 from pickle Chinese cabbage. *International Journal of Biological Macromolecules, 120*(Pt A), 1315–1321. https://doi.org/10.1016/j.ijbiomac.2018.09.019

Zhang, K., Liu, S., Liang, S., Xiang, F., Wang, X., Lian, H., Li, B., & Liu, F. (2024). Exopolysaccharides of lactic acid bacteria: Structure, biological activity, structure-activity relationship, and application in the food industry: A review. *International Journal of Biological Macromolecules, 257*(Pt 2), Article 128733. https://doi.org/10.1016/j.ijbiomac.2023.128733

Zhang, L., Kong, H., Li, Z., Ban, X., Gu, Z., Hong, Y., Cheng, L., & Li, C. (2023). Physicochemical characterizations, α-amylase inhibitory activities and inhibitory mechanisms of five bacterial exopolysaccharides. *International Journal of Biological Macromolecules, 249*, Article 126047. https://doi.org/10.1016/j.ijbiomac.2023.126047

Zhao, D., Jiang, J., Liu, L. N., Wang, S., Ping, W. X., & Ge, J. P. (2021). Haracterization of exopolysaccharides produced by Weissella confusa XG-3 and their potential biotechnological applications. *International Journal of Biological Macromolecules, 178*, 306–315. https://doi.org/10.1016/j.ijbiomac.2021.02.182

Zhao, J., Fu, H., Zhang, Y., Li, M., Wang, D., Zhao, D., Zhang, J., & Wang, C. (2022). Protective effects of Lactobacillus reuteri SJ-47 strain exopolysaccharides on human skin fibroblasts damaged by UVA radiation. *Bioresources and Bioprocessing, 9*(1), 127. https://doi.org/10.1186/s40643-022-00617-0

Zhou, Y., Cui, Y., & Qu, X. (2019). Exopolysaccharides of lactic acid bacteria: Structure, bioactivity and associations: A review. *Carbohydrate Polymers, 207*, 317–332. https://doi.org/10.1016/j.carbpol.2018.11.093

Zhou, Y., Cui, Y., Suo, C., Wang, Q., & Qu, X. (2021). Structure, physicochemical characterization, and antioxidant activity of the highly arabinose-branched exopolysaccharide EPS-M2 from Streptococcus thermophilus CS6. *International Journal of Biological Macromolecules, 192*, 716–727. https://doi.org/10.1016/j.ijbiomac.2021.10.047